

Oxidative dehydrogenation of ethane over some titanates based perovskite oxides

Takashi Hayakawa, Arnfinn G. Andersen^{1,2}, Hideo Orita, Masao Shimizu
and Katsuomi Takehira²

*Oxidation Laboratory, National Chemical Laboratory for Industry, 1-1 Higashi, Tsukuba,
305 Ibaraki, Japan*

Received 30 July 1992; accepted 29 September 1992

A series of perovskite catalysts have been tested for the oxidative dehydrogenation of ethane. The composition of these catalysts covered $\text{CaTi}_{1-x}\text{Fe}_x\text{O}_{3-\delta}$, with $0 \leq x \leq 0.4$, $\text{SrTi}_{1-x}\text{Fe}_x\text{O}_{3-\delta}$, with $0 \leq x \leq 1.0$, as well as mixtures of these. The latter catalysts containing more basic Sr metal showed higher selectivity to ethene than the former catalysts containing Ca. A few catalysts with Co on B-sites in the lattice were tested, but lost their stability above 923 K, resulting in a substantial change in the product selectivity. The perovskites gained activity when Fe was introduced in the lattice to form hypervalent ions (Fe^{4+}) which are believed to play a role in the catalytic activity of these materials.

Keywords: Perovskites; oxidative dehydrogenation; ethane; titanates based catalysts; hypervalency

1. Introduction

The interest in oxidative dehydrogenation of ethane may be limited as the selectivity of such a process can hardly compete with the existing technology, i.e. dehydrogenation process. Nevertheless, an oxidative process still has some advantages as there will be no need for external heating of the reactor, as well as no need to consider equilibrium limitations, and the problem of coking may be reduced with little or no added steam. Furthermore, much attention is paid to the oxidative methane coupling, and oxidative dehydrogenation of ethane will take place as a secondary step in this process. A recent study showed similar properties in oxidative dehydrogenation of ethane and oxidative coupling of methane (OCM) for various oxide catalysts [1].

¹ Permanent address: Senter for Industriforskning, P.O. Box 124 Blindern, 0314 Oslo 3, Norway.

² To whom correspondence should be addressed.

The present study was performed as part of a search for a catalyst for electrochemical conversion of light hydrocarbons, using a zirconia solid electrolyte membrane reactor [2], as previously reported by us [3] and several authors [4]. Usually we use yttria stabilized zirconia (YSZ) as the solid electrolyte, over the anode side of which a thin catalyst film is deposited. A catalyst for this purpose should be a material with mobility for both electrons and oxide ions, and chemical and mechanical stability should be maintained during preparation and operation of the reactor. Furthermore, the catalyst should be able to activate light hydrocarbons. The materials characteristics mentioned are found among some perovskites, and titanates are among the most stable compounds of this class. A recent report also showed that $\text{Ca}_{0.9}\text{Sr}_{0.1}\text{TiO}_3$ has reasonably high catalytic activity for oxidative coupling of methane [5]. Some of the catalysts for oxidative dehydrogenation of ethane [6–8] are also based on perovskites [6,7].

We have carried out a screening of catalysts with a similar composition for oxidative dehydrogenation of ethane. Selected catalysts from this screening will later be used in electrochemical studies. The catalytic results in the present study will be compared with properties like conductivity and the presence of surface carbonate species, as these properties have been suggested by Dubois et al. [9,10] and one of the authors [11] to be important for a similar reaction, namely the oxidative coupling of methane.

2. Experimental

An overview of the catalysts used in the present study is given in fig. 1. The materials have the general formula $\text{Ca}_{1-x}\text{Sr}_x\text{Ti}_{1-y}\text{Fe}_y\text{O}_{3-\delta}$. A few samples

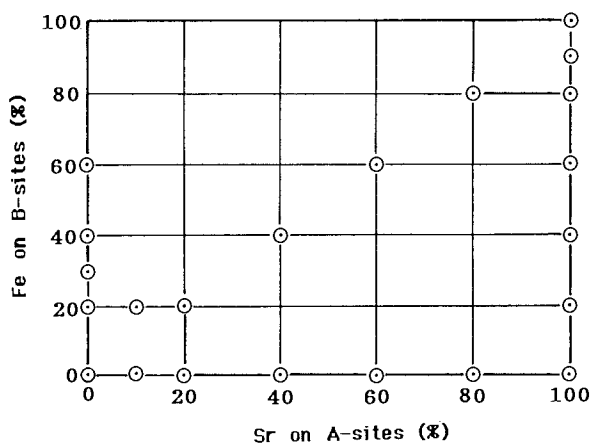


Fig. 1. Illustration of the compositions of samples with the general formula $\text{Ca}_{1-x}\text{Sr}_x\text{Ti}_{1-y}\text{Fe}_y\text{O}_{3-\delta}$ used in the present study. The corners of the figure represent pure ternary oxides (e.g. the lower left corner represents CaTiO_3 and the upper right represents $\text{SrFeO}_{3-\delta}$), while compositions in between the corners have a mixture of the atoms on A- and B-sites in the perovskite. In addition a few samples were tested with Co on B-sites in the perovskites.

where Fe has been replaced with Co will also be included. The structure, homogeneity range and stability, as well as the synthesis of the materials, have been reported separately [12]. An important feature to keep in mind in the following discussion is that the surface area of the titanates was around 15 m²/g, while the surface area of catalysts containing Fe was about 1 m²/g.

All materials have been tested as the catalyst for oxidative dehydrogenation of ethane in a mixture of air (3.0 ℓ/h) and ethane (1.5 ℓ/h, from Takachiho Chemical Industry Co. Ltd.). 330 mg catalyst was dispersed in 2 ml of quartz wool to avoid sintering and clogging of the reactor. The quartz reactor used was U-shaped, with the catalyst bed near the bottom. The inner diameter of the inlet tube was 10 mm and the outlet was 4 mm. Above and below the catalyst bed the reactor was filled with quartz sand. The thermocouple was introduced from above and placed in the middle of the catalyst bed. 0.5 ml of the product gases were sampled immediately after the reactor and injected into a GC for analysis. All the catalyst samples in the present study are, unless otherwise mentioned, calcined at 1123 K for 5 h before catalytic testing.

Catalytic tests were performed as follows: the temperature of the reactor was raised to 773 K in air and the reactant gas mixtures were introduced after a short flushing with N₂. No change in product distribution was observed after 15 min on line. All samples in the following are taken 15 min or more after establishing steady state of the reaction. The temperature was further elevated to 873, 923, 973 and 1023 K and the activity was similarly tested at each reaction temperature. After this, the same catalyst was tested for the OCM reaction [13]. Finally, the whole reactor was quickly removed from the furnace with the reacting gases present, and quenched in cold water in order to preserve any phases stable only under reaction conditions. We presume that the results of the following characterization is representative for the situation even during reactions in ethane, as the influence of the two gas mixtures impose similar effects on the solid state properties of the catalyst.

Characterization of the catalyst was carried out as follows: the powder X-ray diffraction (XRD) diagrams were recorded by using MXP-18 (MAC Science Co.) with Cu K α radiation. Thermal analyses (TGA/DTA) were carried out by using Shimadzu TGA 50 and DTA 50 containing an electrobalance. Diffuse reflectance infrared spectra were recorded by using a JASCO FT/IR 7000 spectrometer.

3. Results and discussion

As a preliminary experiment, the reactor was filled with quartz sand and quartz wool, i.e. without catalyst, and was tested with the same gas mixture as used in the catalytic reaction. Thermal activation of the reaction was observed to play a role above 973 K, but the ethane conversion was still only 5 to 15% of the

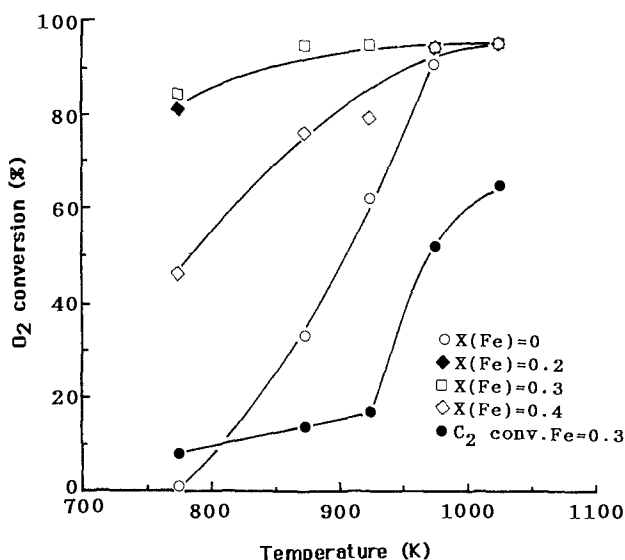


Fig. 2. Oxygen conversion as a function of temperature in a flow of ethane (1.5 ℓ /h) and air (3.0 ℓ /h) over various catalysts of $\text{CaTi}_{1-x}\text{Fe}_x\text{O}_{3-\delta}$. One example of ethane conversion, for $x = 0.3$, is included.

conversion in the presence of catalysts used in this study. The main product in the quartz filled reactor was ethene (> 90%).

3.1. CATALYST BASED ON CaTiO_3

Catalytic features of materials with Fe substituted into B-sites of CaTiO_3 are presented in figs. 2–4. Four samples of $\text{CaTi}_{1-x}\text{Fe}_x\text{O}_{3-\delta}$ with $0 \leq x \leq 0.4$ were used, as the solubility limit of Fe is close to $x = 0.5$ [12,14]. The ethane conversion was similar for all materials, increasing sharply above 923 K, as observed over a typical example catalyst, i.e. $\text{CaTi}_{0.7}\text{Fe}_{0.3}\text{O}_{3-\delta}$ (fig. 2). This is fifty degrees lower than the temperature where thermal activation starts to have a certain impact on the oxidation mechanism. The oxygen conversion was highest for intermediate Fe contents ($x = 0.2$ – 0.3) at low temperature, but in the higher temperature range all samples behave alike (fig. 2). The selectivity for ethene as a function of temperature is shown in fig. 3. A sharp increase was observed for all the catalysts above 873 K. The selectivity to CO was high for CaTiO_3 (48% at 573–673 K, falling to 18% at 973 K), but all Fe containing materials showed low CO selectivity (5% at 573–673 K, rising to 10% above 973 K). The selectivity to CO_2 was highest for intermediate Fe contents, and decreased sharply above 923 K, as shown in fig. 4.

The main feature in this series of experiments seems to be that the catalysts lower the temperature for thermal reaction considerably. Furthermore, the

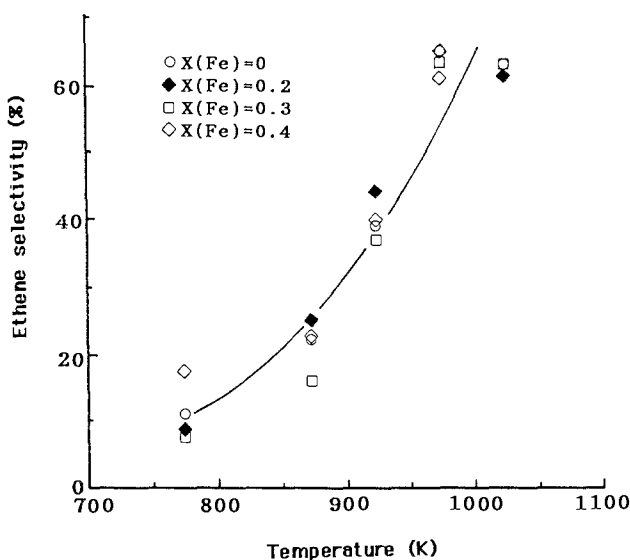


Fig. 3. Ethene selectivity as a function of temperature in a flow of ethane (1.5 ℓ /h) and air (3.0 ℓ /h) over various catalysts of $\text{CaTi}_{1-x}\text{Fe}_x\text{O}_{3-\delta}$.

presence of Fe dramatically changes the selectivity to CO at lower temperatures. Finally, the CO_2 selectivity and the O_2 conversion are high for intermediate Fe contents. The data for p-type and oxide ionic conductivity shown in figs. 5 and 6,

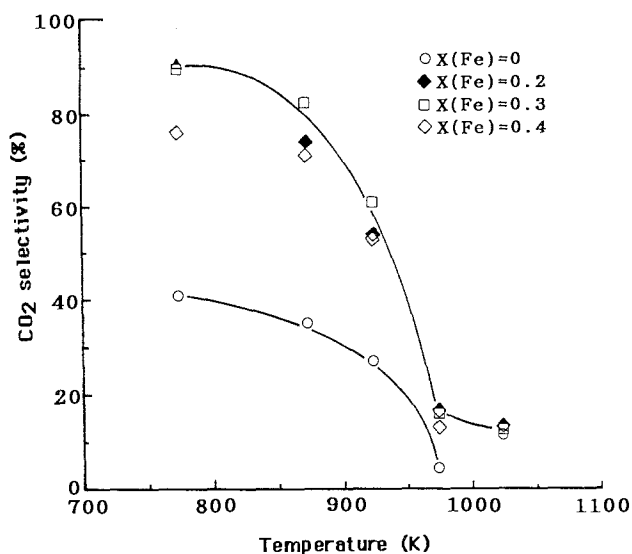


Fig. 4. CO_2 selectivity as a function of temperature in a flow of ethane (1.5 ℓ /h) and air (3.0 ℓ /h) over various catalysts of $\text{CaTi}_{1-x}\text{Fe}_x\text{O}_{3-\delta}$.

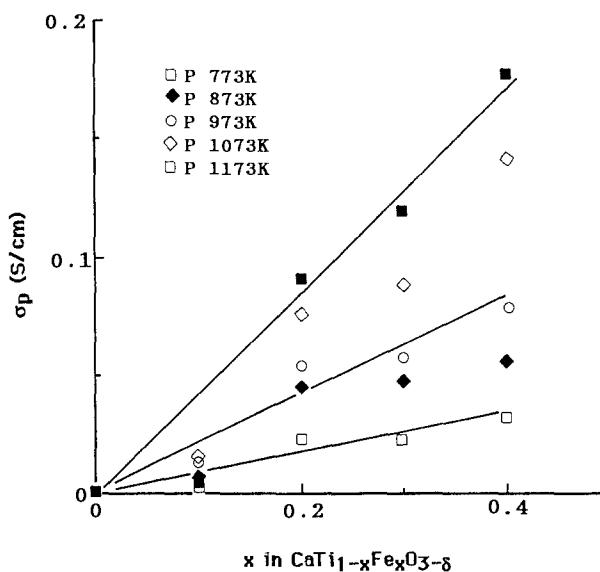


Fig. 5. p-type conductivity as a function of Fe substitution at various temperatures for $\text{CaTi}_{1-x}\text{Fe}_x\text{O}_{3-\delta}$; the data are calculated from a study by Iwahara et al. [14].

respectively, were calculated from a study by Iwahara et al. [14], according to the following equations:

$$\sigma_{\text{O}^{2-}} = t_{\text{ion}} \sigma_{\text{total}} \quad \text{and} \quad \sigma_p = \sigma_{\text{total}} - \sigma_{\text{O}^{2-}},$$

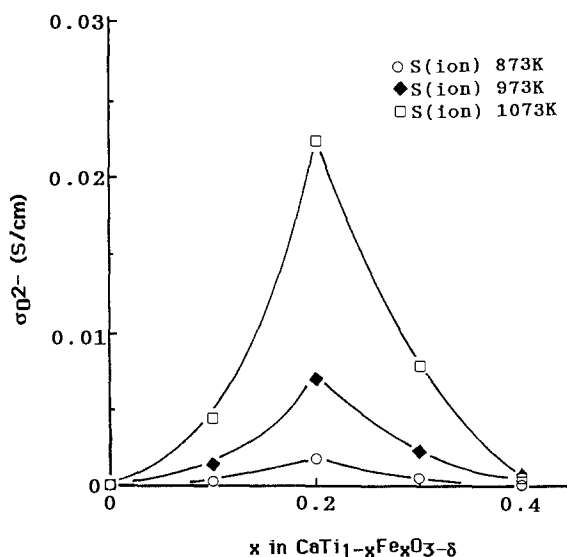


Fig. 6. Oxygen ion conductivity as a function of Fe substitution at various temperatures for $\text{CaTi}_{1-x}\text{Fe}_x\text{O}_{3-\delta}$; the data are calculated from a study by Iwahara et al. [14].

where $\sigma_{\text{O}^{2-}}$ is the conductivity for oxide ions, σ_{total} is the total conductivity, t_{ion} is the ion transport number and σ_{p} is the p-type conductivity. We assume that other charge carriers are of negligible importance.

p-type conductivity increased monotonously with Fe-content and temperature, while the mobility of oxide ions is highest for intermediate compositions. The dependence of the OCM reaction on p-type conductivity, as suggested by Dubois and Cameron [9,10], is not reflected in the product distribution in the present work on ethane. However, there seems to be a correlation between oxide ion conductivity and O_2 conversion (or CO_2 selectivity) at lower temperature (fig. 2 or 4), as both have a maximum at intermediate Fe contents. Thus, high oxide ion conductivity afforded high oxidation activity, suggesting that mobility of lattice oxygen species is important in these catalysts. At higher temperatures, it is likely that desorption of ethene is faster than its deep oxidation to carbon oxides on the catalyst surface, resulting in higher selectivity to C_2 compounds (figs. 3 and 4).

The catalysts used above were studied by diffuse reflectance infrared spectroscopy before and after catalytic testing. None of the materials in the series $\text{CaTi}_{1-x}\text{Fe}_x\text{O}_{3-\delta}$ showed any change in XRD patterns during catalytic testing, but IR revealed changes in the surface. Fig. 7 shows the IR spectrum of $\text{CaTi}_{0.7}\text{Fe}_{0.3}\text{O}_{3-\delta}$ before and after testing. The carbonate band at 1450 cm^{-1} is seen before and after testing, but the main feature is the general “blackening” of the sample after the catalytic test. This phenomena normally occurs when a surface is reduced, or more generally, when a surface becomes conductive. CaTiO_3 showed no carbonate band, and no change during testing. The IR spectrum of $\text{CaTi}_{0.8}\text{Fe}_{0.2}\text{O}_{3-\delta}$ was similar to fig. 7 before testing, but became

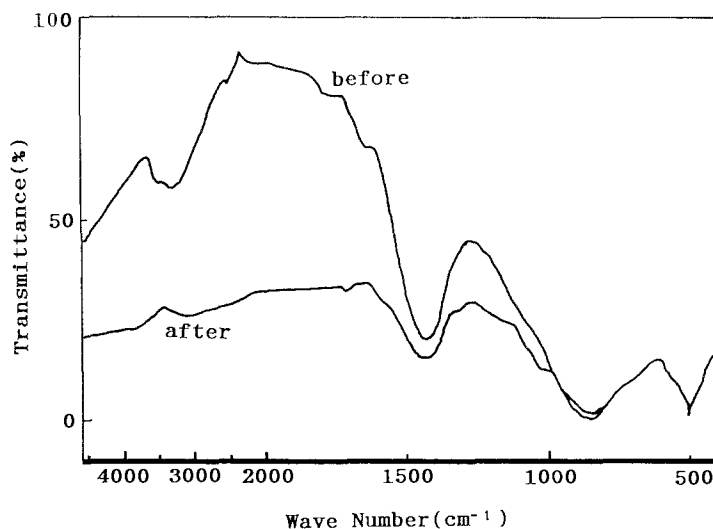


Fig. 7. Diffuse reflectance infrared spectra of $\text{CaTi}_{0.6}\text{Fe}_{0.4}\text{O}_{3-\delta}$ before and after the catalytic testing.

totally “black” during testing. $\text{CaTi}_{0.6}\text{Fe}_{0.4}\text{O}_{3-\delta}$ showed a weaker carbonate band and no change during testing.

The presence of surface carbonate species has been suggested by Dubois and Cameron to be beneficial for the OCM reaction [9,10]. In the present study with ethane, these species are observed over the catalysts which showed low yields of CO and high yields of CO_2 , as well as high O_2 conversions. The “blackening” of the surface is most profound for the samples of intermediate Fe contents. This is somewhat surprising, as the p-type conductivity increases monotonously with Fe-doping. Thus, the surface conductivity of this perovskite does not completely follow the bulk properties of the oxide. Another explanation could be that the reducibility of the surface for some reason is highest for intermediate compositions.

3.2. CATALYSTS BASED ON SrTiO_3

Results from catalytic testing of $\text{SrTi}_{1-x}\text{Fe}_x\text{O}_{3-\delta}$ are found in figs. 8–11. As observed for the previously discussed Ca compounds, oxygen conversion at temperatures below 973 K was drastically increased when Fe was introduced in the lattice despite the reduction in surface area. The ethane conversion, as shown in fig. 8, increased with temperature for all catalysts, but the variation among the catalysts was complex. However, SrTiO_3 behaved similarly to the Ca compounds discussed above (see fig. 2). The ethene selectivity increased with the Fe content, as seen in fig. 9, possibly with a maximum for $x = 0.8$. At this point and 1123 K, an ethene yield of 52% was obtained. As for the Ca

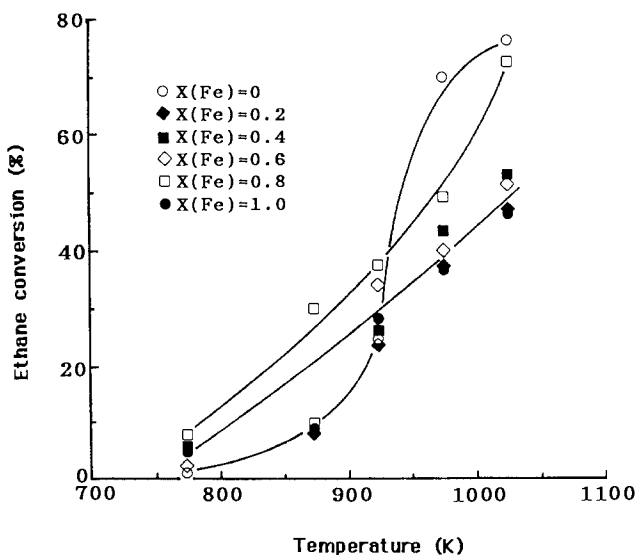


Fig. 8. Ethane conversion as a function of temperature in a flow of ethane (1.5 ℓ /h) and air (3.0 ℓ /h) over various catalysts of $\text{SrTi}_{1-x}\text{Fe}_x\text{O}_{3-\delta}$.

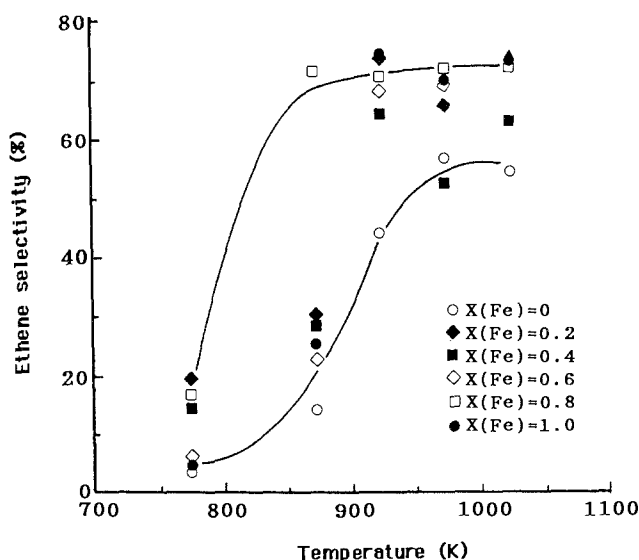


Fig. 9. Ethene selectivity as a function of temperature in a flow of ethane (1.5 ℓ /h) and air (3.0 ℓ /h) over various catalysts of $\text{SrTi}_{1-x}\text{Fe}_x\text{O}_{3-\delta}$.

compounds, the CO selectivity was high for the sample without Fe (fig. 10), while the CO_2 selectivity was low for the same catalyst (fig. 11). In these oxidations over $\text{SrTi}_{1-x}\text{Fe}_x\text{O}_{3-\delta}$ ($x > 0$), CH_4 and higher hydrocarbons (C_{3+}) were detected. The selectivities to CH_4 increased with temperature for all catalysts, reaching about 10% at 1023 K. The maximum value was obtained

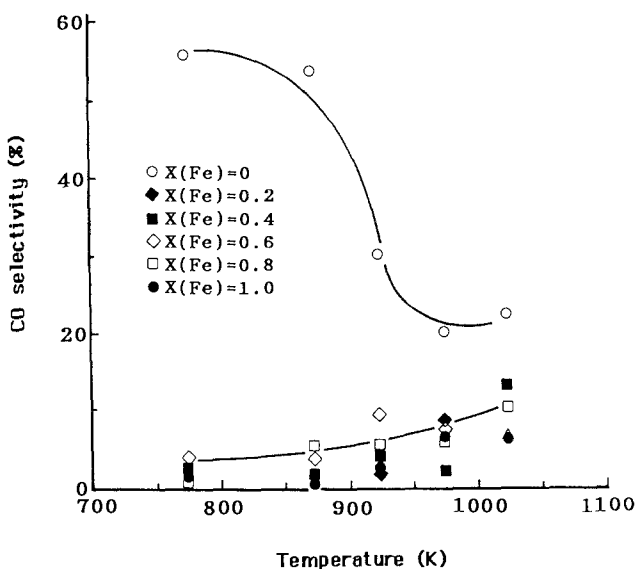


Fig. 10. CO selectivity as a function of temperature in a flow of ethane (1.5 ℓ /h) and air (3.0 ℓ /h) over various catalysts of $\text{SrTi}_{1-x}\text{Fe}_x\text{O}_{3-\delta}$.

around $x = 0.8$. The selectivity to C_{3+} hydrocarbons seemed to reach a maximum of about 8% at 973 K. The product distribution was complex and varied between the catalysts. However, it is clear that, for catalysts containing Fe, C–C bond fission and recombination occurred during the reaction.

A clear change in the ethene/ CO_2 ratio in the product stream was seen at 873 K for $SrTi_{1-x}Fe_xO_{3-\delta}$ (figs. 9 and 11), and at 923 K for $CaTi_{1-x}Fe_xO_{3-\delta}$ (figs. 3 and 4). Both temperatures are below that of thermal activation of ethane. However, no evidence for this change of behaviour has been found in physical properties, like conductivity, nor in DTA/TG studies. Since strontium is more basic than calcium, it is likely that a basic product, ethene, can be more quickly desorbed from $SrTi_{1-x}Fe_xO_{3-\delta}$ than from $CaTi_{1-x}Fe_xO_{3-\delta}$, resulting in the higher selectivity for ethene at lower temperature over $SrTi_{1-x}Fe_xO_{3-\delta}$.

To the knowledge of these authors, no study that can separate the various types of conductivities at elevated temperature has been published for the system $SrTi_{1-x}Fe_xO_{3-\delta}$. However, this mixed oxide should be a fairly good conductor for oxygen ions. Still, p-type conductivity is dominating for $x > 0.2$, and it is probably monotonously increasing with x and temperature for $x > 0.2$ [15–17]. There is also a complex relation between conductivity and oxygen content for $SrFeO_{3-\delta}$, giving a good conductor at high oxygen contents (i.e. high oxygen partial pressures). In the present study, one may still conclude that the ethene selectivity increases with p-type conductivity.

The IR spectrum of $SrTiO_3$ showed no carbonate species before the catalytic test, and a weak carbonate signal after the test. All samples containing Fe, however, showed a clear carbonate band. The sample $SrTi_{0.8}Fe_{0.2}O_{3-\delta}$ became

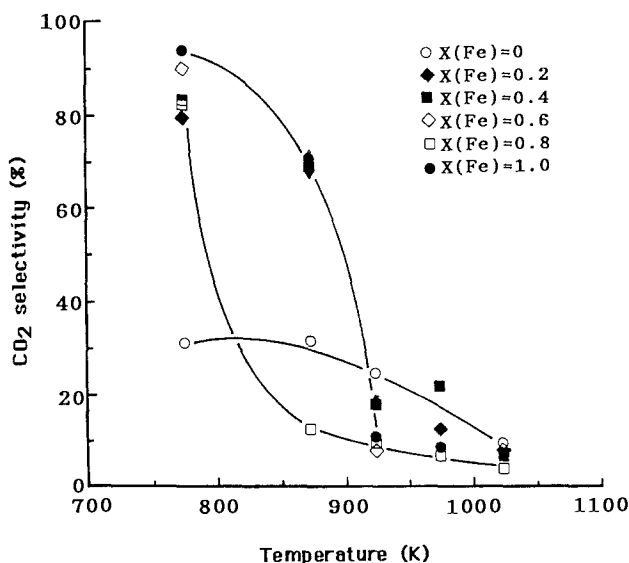


Fig. 11. CO_2 selectivity as a function of temperature in a flow of ethane (1.5 ℓ/h) and air (3.0 ℓ/h) over various catalysts of $SrTi_{1-x}Fe_xO_{3-\delta}$.

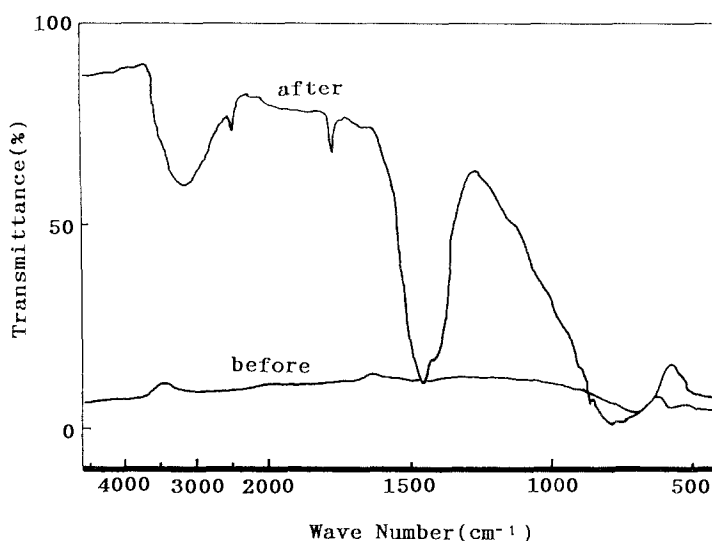


Fig. 12. Diffuse reflectance infrared spectra of $\text{SrTi}_{0.2}\text{Fe}_{0.8}\text{O}_{3-\delta}$ before and after the catalytic testing.

“IR-black” during testing, as did the similar Ca containing samples. The Sr compounds with 40 and 60% Fe substitution did not show any particular blackening. Fig. 12 shows the IR spectrum of $\text{SrTi}_{0.2}\text{Fe}_{0.8}\text{O}_{3-\delta}$. This sample was “IR-black” before the catalytic test, and not after the test. Thus, the surface must have best conductivity in an oxidizing atmosphere, and the same is the case for $\text{SrFeO}_{3-\delta}$. This fits well with the conductivity data on $\text{SrFeO}_{3-\delta}$ of MacChesney et al. [17], which showed highest conductivity for small values of δ . The difference in oxygen content of the present catalyst before and after testing has been studied separately [12]. However, as for the Ca compounds, this “IR-blackening” of the surface cannot be totally explained by the bulk properties of the perovskite.

From the literature on $\text{SrTi}_{1-x}\text{Fe}_x\text{O}_{3-\delta}$, it is known, at least for high values of x , that a large amount of the iron in the lattice is presents as Fe^{4+} [15–17]. The lattice is moreover compensated by vacancies in the oxygen lattice. We assume that these hypervalent Fe ions are metastable and would play an important role in hydrocarbon oxidation. Samples with substitution of the A-sites (i.e. with mixtures of Ca and Sr ions) showed no specific features, but could be interpreted as interpolations of the two series of materials discussed here.

3.3. CATALYSTS CONTAINING Co

Fig. 13 shows the data obtained by a catalyst containing Co on B-sites ($\text{Ca}_{0.8}\text{Sr}_{0.2}\text{Ti}_{0.8}\text{Co}_{0.2}\text{O}_{3-\delta}$). The conversions of ethane and oxygen showed similar

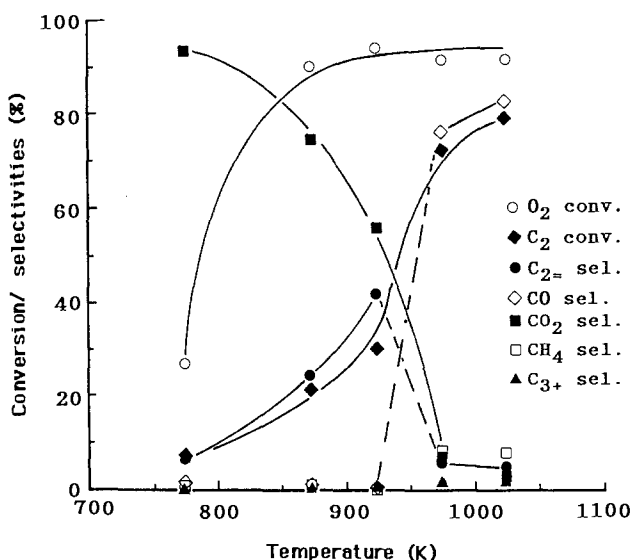


Fig. 13. Ethane and oxygen conversion and selectivities to ethene, CO and CO₂ as a function of temperature for Ca_{0.8}Sr_{0.2}Ti_{0.8}Co_{0.2}O_{3-δ}.

trends with the reaction temperature to the data obtained over the catalysts discussed above. The selectivity to CO₂ decreased with temperature from nearly 100% at 773 K to nearly nil above 973 K. The selectivity to ethene increased steadily to above 40% at 923 K; above which the selectivity to ethene was lost and CO became the main product. The same phenomenon was observed with 60% substitution in both A- and B-lattices. In this experiment, the ethene selectivity reached 72% at 923 K; above this temperature, CO took over as the main product with the same selectivity. After catalytic testing, XRD showed a complex diagram, including some CoO.

The observed changes in selectivities of Co containing catalysts are probably due to a phase separation in the surface of these materials. The catalysts were shown to partly decompose during catalytic testing by XRD. Furthermore, the decomposition both in air (1238 K) and N₂ (1098 K) was observed by DTA/TGA. The decomposition in the reducing mixture of ethane and air is likely to occur at lower temperatures, and could well be the reason for the observed change in selectivity. The DTA/TGA studies in N₂ are illustrated in fig. 14. TGA shows two steps of weight loss, and DTA shows three peaks in the same temperature region, reflecting two steps in decomposition and an additional phase transformation. After these experiments in N₂, XRD showed the presence of CoO and CaO in addition to the perovskite. Similar studies in air showed two peaks of weight loss and one broad DTA signal. According to XRD, the material still consisted of perovskite after the experiments in air. The thermal behavior of this material is complex. In the literature, the complex behavior of SrCoO_{3-δ} has been described by Takeda et al. [18].

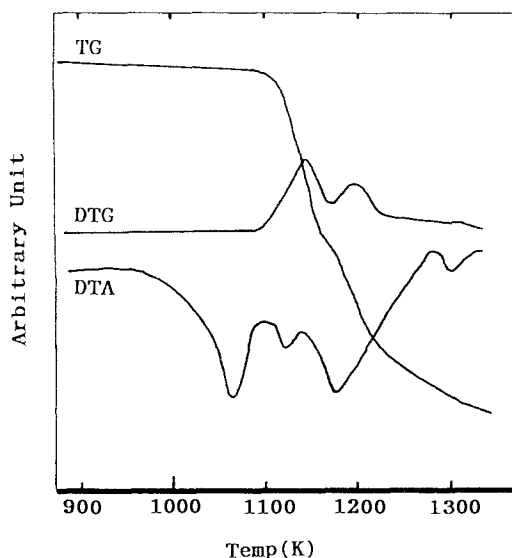


Fig. 14. DTA/TG/TGA illustrating the decomposition of $\text{Ca}_{0.4}\text{Sr}_{0.6}\text{Ti}_{0.4}\text{Co}_{0.6}\text{O}_{3-\delta}$ during heating in N_2 at a rate of 10 K/min.

Cobalt catalysts are known to be fairly good for the reforming reaction. In the present study, H_2O can be formed during the oxidative reaction, and one could argue that this steam is consumed in a reforming reaction with ethane/ethene to form CO and H_2 in a secondary reaction. However, cobalt may also be used in the same way as nickel as a catalyst for partial oxidation of hydrocarbons to synthesis gas at high temperatures (> 1473 K). Vernon et al. [19] recently reported that partial oxidation of methane can be accelerated over lanthanide ruthenium oxide catalysts at temperatures of only 1050 K. It was also reported by Uchijima et al. [20] that various metals such as Rh, Ru, Ni and Pt supported on SiO_2 catalyze this oxidation at further low temperatures of 900 K. In both cases, the reaction mechanism is not yet elucidated. In fact, all ethene disappeared from the products when the CO production started in the present work. Moreover, the sudden change in selectivity from ethene at lower temperature to CO at 973 K was accompanied by a substantial production of hydrogen, though our gas chromatographs were not equipped for quantitative analysis of the amount of hydrogen. In the present study, we can therefore conclude that the catalyst after the decomposition promotes the direct, partial oxidation of ethane to synthesis gas.

4. Conclusion

Several perovskite catalysts have been tested for oxidative dehydrogenation of ethane. In the series of $\text{CaTi}_{1-x}\text{Fe}_x\text{O}_{3-\delta}$, with $0 \leq x \leq 0.4$, the introduction of

Fe in the lattice induced a higher activity of the catalyst. The catalytic results are in fair agreement with the hypothesis for the OCM reaction, i.e. importance of both p-type conductivity and carbonate formation in the catalyst. The same may be said for the series of $\text{SrTi}_{1-x}\text{Fe}_x\text{O}_{3-\delta}$, with $0 \leq x \leq 1.0$. In the latter case, the maximum yield for ethene of 52% occurred at 1023 K with $x = 0.8$. The catalysts were stable under testing conditions, but a change in the surface states was observed by IR. Catalysts containing Co in the B-sites were not stable above 923 K and did not keep the selectivity to ethene.

Acknowledgement

The grant from Agency of Industrial Science and Technology, MITI, is highly acknowledged by one of the authors, AGA, to do this work in NCLI.

References

- [1] E.M. Kennedy and N.W. Cant, *Appl. Catal.* 75 (1991) 321.
- [2] A.G. Andersen, T. Hayakawa, H. Orita, M. Shimizu and K. Takehira, to be published.
- [3] T. Hayakawa, T. Tsunoda, H. Orita, T. Kameyama, H. Takahashi, K. Takehira and K. Fukuda, *J. Chem. Soc. Chem. Commun.* (1986) 961;
T. Hayakawa, T. Tsunoda, H. Orita, T. Kameyama, H. Takahashi, K. Fukuda and K. Takehira, *J. Chem. Soc. Chem. Commun.* (1987) 780;
T. Hayakawa, T. Tsunoda, H. Orita, T. Kameyama, M. Ueda, K. Fukuda and K. Takehira, *J. Chem. Soc. Chem. Commun.* (1988) 1593.
- [4] C.B. Choudhary, H.S. Maiti and E.C. Subbarao, in: *Solid Electrolytes and Their Applications*, ed. E.C. Subbarao (Plenum Press, New York, 1980) pp. 1–80;
K. Ohtsuka, S. Yokoyama and A. Morikawa, *Chem. Lett.* (1985) 319;
K. Ohtsuka, K. Suga and I. Yamanaka, *Chem. Lett.* (1988) 317;
E. Eng and M. Stoukides, *Catal. Rev. Sci. Eng.* 33 (1991) 375.
- [5] Y. Xu, H. Lui, J. Huang, Z. Lin and X. Guo, *Proc. of the 3rd China–Japan Symp. on Coal and C1 Chemistry*, Kunming, China, Oct. 29–Nov. 1, 1990, p. 449.
- [6] O.J. Velle, A.G. Andersen and K.-J. Jens, *Catal. Today* 6 (1990) 567.
- [7] J. Kolts, US Patent 4,368,344 (1983).
- [8] J.B. Kimble, US Patent 4,476,344 (1984).
- [9] J.-L. Dubois and C.J. Cameron, *Appl. Catal.* 67 (1990) 49.
- [10] J.-L. Dubois and C.J. Cameron, *Chem. Lett.* (1991) 1089.
- [11] T. Norby and A.G. Andersen, *Appl. Catal.* 71 (1991) 89.
- [12] A.G. Andersen, T. Hayakawa, T. Tsunoda, H. Orita, M. Shimizu and K. Takehira, *Catal. Lett.*, submitted.
- [13] A.G. Andersen, T. Hayakawa, T. Tsunoda, H. Orita, M. Shimizu and K. Takehira, to be published.
- [14] H. Iwahara, T. Esaka and T. Mangahara, *J. Appl. Electrochem.* 18 (1988) 173.
- [15] T.R. Clevenger Jr., *J. Am. Ceram. Soc.* 46 (1963) 207.
- [16] L.H. Brixner, *Mater. Res. Bull.* 3 (1968) 299.
- [17] J.B. MacChesney, R.C. Sherwood and J.F. Potter, *J. Chem. Phys.* 43 (1965) 1907.

- [18] Y. Takeda, R. Kanno, T. Takeda, O. Yamamoto, M. Takano and Y. Bando, *Z. anorg. allg. Chem.* 540/541 (1986) 259.
- [19] A.T. Ashcroft, A.K. Cheetham, J.S. Foord, M.L.H. Green, C.P. Grey, A.J. Murrell and P.D.F. Vernon, *Nature* 344 (1990) 319;
P.D.F. Vernon, M.L.H. Green, A.K. Cheetham and A.T. Ashcroft, *Catal. Lett.* 6 (1990) 181.
- [20] J. Nakamura, S. Umeda, K. Kubushiro, T. Ohashi, K. Kunitori and T. Uchijima, *Shokubai* 33 (1991) 99.